Available online at www.sciencedirect.com
SCIENCE DIRECT®
Journal of Chromatography A, 1026 (2004) 47–55
JOURNAL OF CHROMATOGRAPHY A
www.elsevier.com/locate/chroma

Solvent gradient operation of simulated moving beds 2. Langmuir isotherms

Stefanie Abel [a], Marco Mazzotti [a,*], Massimo Morbidelli [b]

[a] *ETH Swiss Federal Institute of Technology Zurich Institute of Process Engineering, Sonneggstrasse 3, CH-8092 Zurich, Switzerland*
[b] *ETH Zurich, Institute for Chemical- and Bio-engineering, CH-8093 Zurich, Switzerland*

Received 19 June 2003; accepted 11 November 2003

Abstract

Simulated Moving Bed separations of enantiomers or fine chemicals are usually carried out in the isocratic mode, i.e. by applying the same operating conditions (temperature, pressure, mobile phase composition, pH) in the whole SMB unit. However, it has been recently recognized that by properly modulating operating conditions in the SMB sections, i.e. Sections 1-4 normally, separation performance in terms of productivity and solvent consumption can be significantly improved. In this work, we study solvent gradient SMB (SG–SMB) operation, where the concentration of a modifier in the main solvent constituting the mobile phase is adjusted along the SMB unit, so as to have weaker retention of the species to be separated in the first two sections, and stronger retention in Sections 3 and 4. Overload chromatographic conditions are considered, where the adsorption behavior is characterized by a nonlinear competitive adsorption isotherm, e.g. a binary Langmuir isotherm. Design criteria to achieve complete separation are developed in the frame of the equilibrium theory of chromatography. The theoretical findings are discussed in view of typical effects of the modifier concentration on retention times and solubility of the species to be separated, and an overall assessment of the SG–SMB technology is attempted.

Keywords: Solvent gradients; Simulated moving bed chromatography; Preparative chromatography; Adsorption isotherms; Langmuir isotherms; Ionone

1. Introduction

Chromatographic separations can be carried out in a continuous way by applying the multicolumn Simulated Moving Bed (SMB) technology, which has been extremely successful in the last ten years particularly when applied to chiral separations in the fine chemical and pharmaceutical industries [1]. New applications to biotechnology related separations are envisaged [2].

Recent developments in the field of SMB have highlightened the possibility of further improving the separation performance by applying non-standard operation modes. On the one hand, schemes where additional operational degrees of freedom are available have been proposed, such as the VARICOL® process where ports and columns are switched in an asynchronous manner [3,4], or the POWERFEED process where the internal and external flowrates are varied during the time period between two successive port switches [5–7]. On the other hand, it has been proposed to optimize each SMB section separately, by tuning operating conditions such as temperature [8], pressure in supercritical applications [9–11], or the mobile phase composition [12–15]. The basic idea is to reduce the retention times in Sections 1 and 2, i.e. from the solvent inlet to the extract and the feed port, and to increase those in Sections 3 and 4, i.e. from the feed port to the raffinate and then the solvent inlet.

This work deals with the last approach, i.e. the solvent gradient SMB (SG–SMB) operation. This can be applied when a mixture of solvents is used as mobile phase, and it is realized by having different compositions in the desorbent stream fed to Section 1 and in the feed stream. In this case, a True Moving Bed (TMB) unit, where the solid and the fluid phase move indeed countercurrently, attains the mobile phase composition profile illustrated in Fig. 1, where x represents the volume fraction of the weaker of the two solvents constituting the binary desorbent mixture, which is referred to in the following as the modifier. It is worth noting that we make the important assumption that neither the main solvent nor the modifier interact with the stationary phase. In Fig. 1,

* Corresponding author. Tel.: +41-1-6322456; fax: +41-1-6321141.
E-mail address: mazzotti@ivuk.mavt.ethz.ch (M. Mazzotti).

0021-9673/$ – see front matter © 2003 Elsevier B.V. All rights reserved.
doi:10.1016/j.chroma.2003.11.054

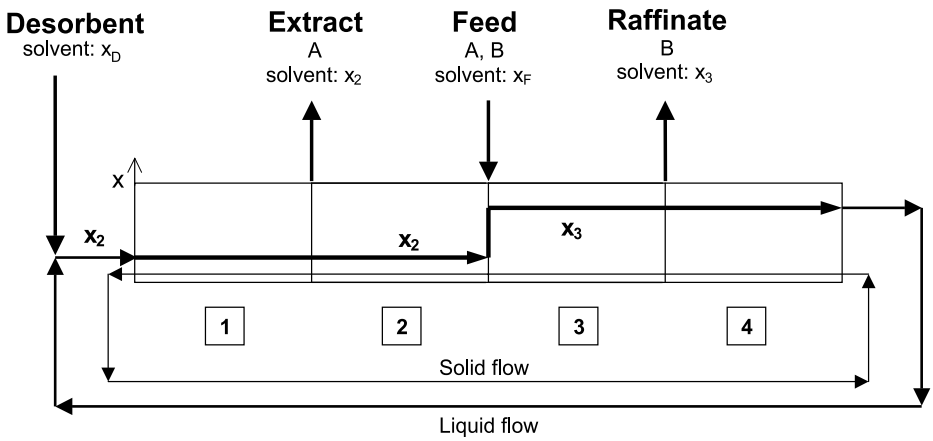

Fig. 1. Scheme of a TMB and the corresponding mobile phase composition profile in a SG–TMB unit where the external solvent compositions are x_D and x_F, with $x_D \le x_2 \le x_3 \le x_F$.

it is also implicitly assumed that a larger modifier concentration, e.g. x_3 as compared to x_2, leads to stronger retention. Longer retention times in Sections 3 and 4 than in Sections 1 and 2 are indeed required for an improvement of the separation performance with respect to isocratic SMB [14]. In the first paper of this series [14], design and optimization criteria have been developed for the SG–SMB in the case where the species to be separated, the more retained component A and the less retained solute B, follow a linear chromatographic behavior, i.e. their adsorption isotherms are linear:

$$q_i = H_i c_i \quad (i = \mathrm{A}, \mathrm{B}), \tag{1}$$

where c_i and q_i are the fluid and adsorbed phase concentrations, respectively, and H_i is the Henry's constant. Such analysis was carried out in the frame of the so called Triangle Theory, whereby two basic assumptions are made. First, the SMB unit is considered equivalent to the TMB unit; the TMB unit achieves a steady state regime, which is not accessible to the SMB unit that can attain only a cyclic steady state behavior due to its port switch mechanism. The SMB-TMB equivalence requires that the following equivalence relationships between SMB and TMB flowrates, i.e. Q_j^{SMB} and Q_j^{TMB}, and between switch time, t^*, in the SMB unit and solid velocity in the TMB unit, Q_s, be fulfilled [14]:

$$\frac{V}{t^*} = \frac{Q_s}{1-\varepsilon_b} \tag{2}$$

$$Q_j^{\mathrm{SMB}} = Q_j^{\mathrm{TMB}} + \frac{Q_s \varepsilon}{1-\varepsilon} \tag{3}$$

Second, the local equilibrium model is adopted to describe the behavior of the chromatographic columns [16]. In this framework, the key operating parameters are the flow rate ratios m_j ($j = 1, \ldots, 4$), defined as:

$$m_j = \frac{Q_j^{\mathrm{SMB}}(t^* - V\varepsilon)}{V(1-\varepsilon)} \tag{4}$$

In this work, we extend the previous linear analysis to the case of systems following the nonlinear, competitive Langmuir isotherm. This extension is needed because in SMB practice it is necessary to operate at high feed concentration in order to increase throughput, i.e. under overload conditions where the assumption of linear, decoupled isotherms does not apply. The chiral separation of α-ionone enantiomers has been selected to illustrate the concepts and methods introduced in this work [14,17,18]. These are separated on a cyclodextrin based chiral stationary phase using methanol as main solvent and water as modifier. Since α-ionone enantiomers are more soluble in methanol than in water, increasing the water fraction in the mobile phase leads to longer retention times, as implied in Fig. 1 [14].

2. Solubilities and adsorption isotherms

In general, changing the mobile phase composition, i.e. the modifier concentration or the pH of the solution or its ionic strength, has a major effect both on the competitive, nonlinear adsorption behavior of the solutes under overload conditions and on their solubility. In principle, when varying the mobile phase composition, one should expect different patterns of behavior obtained by combining opposite trends in the two properties above, i.e. increasing or decreasing retention and increasing or decreasing solubility. In practice, retention and solubility are related, even though such relationship may be difficult to describe quantitatively. In the following we consider the case of the enantiomers of α-ionone in a mixed methanol/water mobile phase, to be separated on a cyclodextrin based Nucleodex-β-PM column (Macherey-Nagel, Düren, Germany) at 20 °C. This system is representative of a rather large class of systems, where increasing solubility (in methanol-rich mobile phases) implies decreasing retention, and vice versa.

2.1. Solubility

The solubility of the α-ionone racemate as a function of the mobile phase composition has been measured at 20 °C.

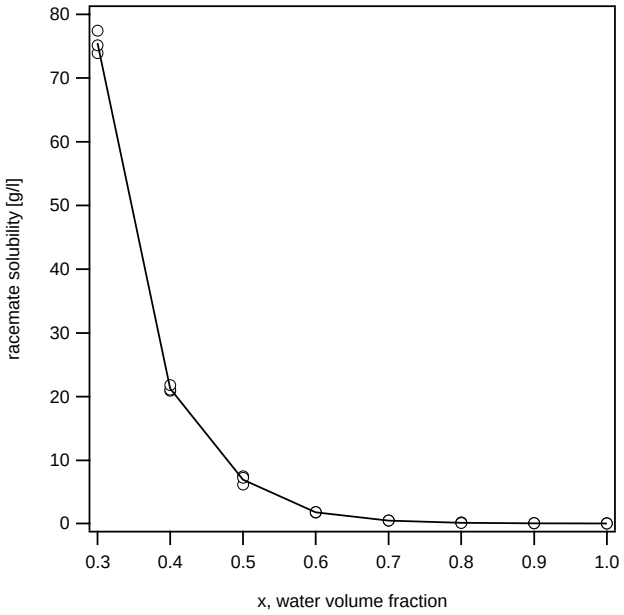

Fig. 2. Solubility of the racemate of α-ionone in methanol/water at 20 °C depending on the solvent composition.

This was done by preparing solvent mixtures with different water content, and saturating them with α-ionone. Pure α-ionone is liquid at 20 °C, thus in order to provide a large interface for mass transfer, the samples were shaken until a raw emulsion was formed and left for 24 h at 20 °C in a water quench. To break the emulsion into a two-phase-system, centrifugation was applied if necessary, and the α-ionone concentration in the solution could be determined by HPLC measurement. From the results illustrated in Fig. 2, it is clear that solubility is quite high in methanol and decreases sharply when adding water to the solution; α-ionone is practically insoluble for $x \geq 0.7$.

2.2. Nonlinear competitive adsorption isotherms

In order to characterize the nonlinear competitive retention behavior of the α-ionone enantiomers as a function of the mobile phase composition, a series of pulse chromatograms of the α-ionone racemate has been measured at 20 °C. These have been performed at various water (modifier) volume fraction values in the mobile phase, i.e. $x = 0.2$, 0.3, 0.4 and 0.5, and at various solute concentrations and amounts injected. The obtained chromatograms show that the retention times of the peak maxima decrease when the amount injected increases, as expected for a Langmuir-type isotherm, whereas the shape of the peaks deviates from the standard Langmuirian behavior. In the following we do not try to capture the detailed behavior of this system, which most likely is rather complex, and we proceed instead by using a standard competitive langmuir isotherm, also based on previous results [8]. In order to highlight the dependence of the adsorption isotherm parameters on the mobile phase composition the following isotherm has been used:

$$q_i(x) = \frac{H_i(x)c_i}{1 + k_A(x)c_A + k_B(x)c_B} \quad (i = A, B), \tag{5}$$

where H_i and k_i are the Henry's constant and the adsorption equilibrium constant, respectively, while A and B refer to (*R*)-(+) α-ionone and to (*S*)-(-) α-ionone, respectively.

The dependence of H_i and k_i on the mobile phase composition can be described in the range of $x \leq 0.85$ through the following equations:

$$H_i(x) = \frac{H_i(0)}{(1 + h_i x)^{n_i}} \quad (i = A, B) \tag{6}$$

$$k_i(x) = k_i(0) \exp\left(\frac{x}{a_i}\right) \quad (i = A, B) \tag{7}$$

where $H_A(0) = 0.32$, $H_B(0) = 0.26$, $h_A = -1.13$, $h_B = -1.17$, $n_A = 5.80$, $n_B = 5.33$, $k_A(0) = 1.48 \times 10^{-5}$ ml/g, $k_B(0) = 2.96 \times 10^{-5}$ ml/g, $a_A = 4.38 \times 10^{-2}$ and $a_B = 4.93 \times 10^{-2}$.

The relationships above indicate that as the water content in the mobile phase increases, the solutes are adsorbed more strongly, the maximum loading capacities (H_i/k_i) decrease, and therefore the nonlinear character of the adsorption isotherm increases.

3. Operating conditions for complete separation in nonlinear SG–SMBs

The temperature or pressure levels in a temperature gradient or pressure gradient simulated moving bed unit can be controlled independently through a device, either a heat exchanger or a back pressure regulator, that does not affect directly the SMB internal flow rates. On the contrary, the mobile phase composition in the solvent gradient SMB unit, e.g. the modifier concentrations x_2 and x_3 in Fig. 1, depend not only on the composition of the external streams, i.e. desorbent and feed, but also on the internal flow rates. To clarify this, let us first consider the closed loop TMB unit illustrated in Fig. 1. Given the modifier concentrations x_D and x_F in the desorbent and feed streams, respectively, the modifier levels x_2 and x_3 are related to the external flow streams through the following material balances at the desorbent and feed nodes:

$$x_2 Q_1^{TMB} = x_D Q_D + x_4 Q_4^{TMB} \tag{8}$$

$$x_3 Q_3^{TMB} = x_F Q_F + x_2 Q_2^{TMB} \tag{9}$$

where Q represents volume flow rates, and for the sake of simplicity volume changes upon mixing are neglected. Let us now consider an open loop unit, where the flow stream leaving Section 4 is discarded and not recycled to Section 1. In this configuration, the mobile phase composition in Sections 1 and 2 is the same as that in the desorbent stream. Accordingly, $x_2 = x_D$ replaces Eq. (8), whereas Eq. (9) still applies to describe the mass balance at the

feed node. It is worth noting that the modifier concentration profiles drawn in Fig. 1 apply only to TMB units, whereas in a SMB unit such concentration values undergo variations due to port switching [14]. In this section we derive criteria for the choice of complete separation operating conditions in the frame of equilibrium theory with reference to a TMB unit, i.e. following a similar approach as in Part I [14], but for the more realistic case of nonlinear isotherms.

3.1. The 'open loop'-configuration

For a nonlinear system a similar procedure can be followed to construct the complete separation region in the (m_2, m_3) plane as in the linear case [14]. For a given pair of (x_2, x_3) modifier concentration values, a triangle-shaped region such as the one drawn in Fig. 3 can be obtained, by considering that different isotherms apply in the different sections of the unit. The specific example considered in Fig. 3 refers to the separation of the α-ionone enantiomers with $x_2 = 0.3$ and $x_3 = 0.34$, and a total racemate feed concentration, $c_T^F = 6$ g/l. By considering an open loop configuration, $x_D = x_2 = 0.3$, and only the points in the triangle-shaped region fulfilling the feed node material balance (9) for the given feed concentration, $x_F = 0.5$ in Fig. 3, are to be considered. These belong to the broken operating line in Fig. 3, obtained by combining Eqs. (4) and (9):

$$m_3(x_F - x_3) = m_2(x_F - x_2), \tag{10}$$

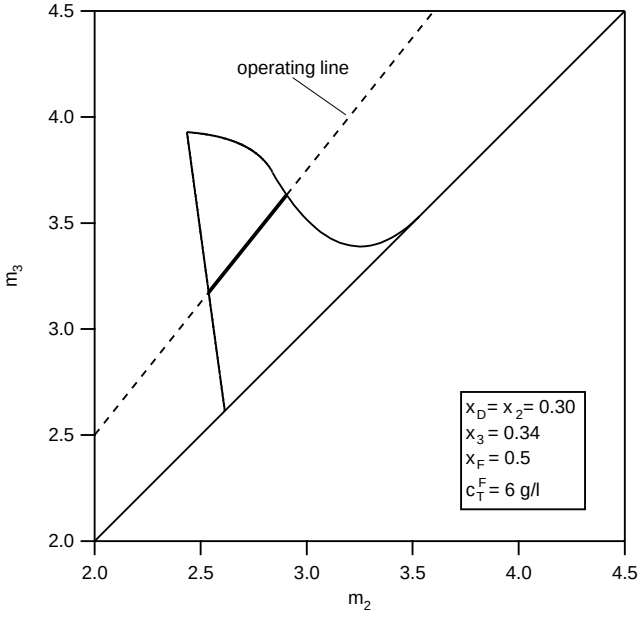

Fig. 3. Nonlinear complete separation region in the (m_2, m_3) plane for a fixed pair (x_2, x_3) for an open-loop configuration, and the operating line given by Eq. (10). Only the segment of the operating line which lies inside the separation area provides accessible operating points for the solvent gradient separation.

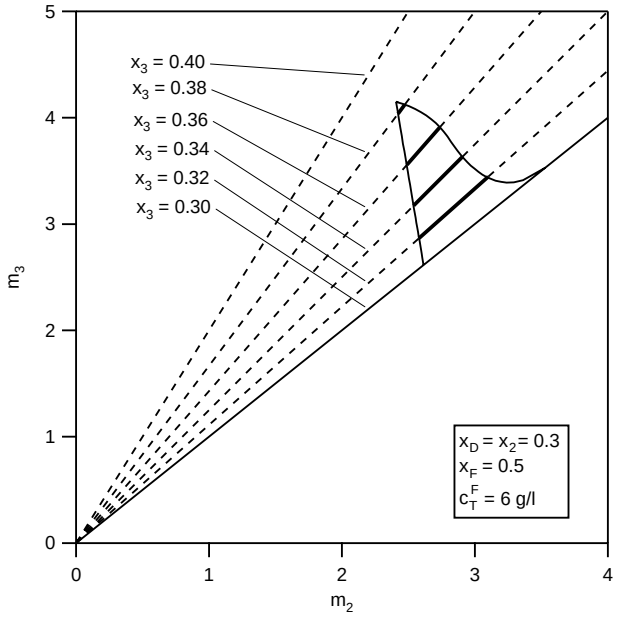

Fig. 4. Operating lines (Eq. (10)) for constant $x_2 = 0.3$, and $x_3 = 0.3$, 0.32, 0.34, . . . , 0.4. Only the solid sections of the operating lines belong to the complete separation region for $x_2 = 0.2$. Same for both linear and nonlinear isotherm, it is obtained by combining all the solid segments.

whose intersecting segment (see Fig. 3) with the complete separation area comprises all points that guarantee complete separation, and are also compatible with the solvent gradient mode operation for the given values x_D, x_3 and x_F.

By repeating this procedure for various values of x_3, while keeping x_D and x_F constant, we get a set of segments for all feasible x_3 values, which can be assembled to form the complete separation region for the given x_D and x_F values in the (m_2, m_3) plane, shown in Fig. 4

Contrary to the linear case, such a region depends on the concentration of the components to be separated in the feed stream, and therefore on the total racemate concentration c_T^F. The effect of c_T^F on the shape and position of the complete separation region, for the given x_D and x_F values, is illustrated in Fig. 5. It can be seen that the area of complete separation shrinks as the feed concentration increases, and the vertex shifts to the left towards lower m_2 values, whereas the intersections with the diagonal do not change.

Let us consider Fig. 5 in view of the following generally accepted definition of productivity for an SMB achieving complete separation of the components in the feed mixture [16]:

$$\mathrm{PR} = \frac{Q_F c_T^F}{n_{col} V} = \frac{(m_3 - m_2)(1-\varepsilon) c_T^F}{n_{col} t^*} \tag{11}$$

It is seen that the productivity is proportional to the product of the total feed concentration, c_T^F, by the distance of the operating point from the diagonal of the (m_2, m_3) plane. In the particular case under examination in Fig. 5, it can be shown that the maximum productivity increases with c_T^F,

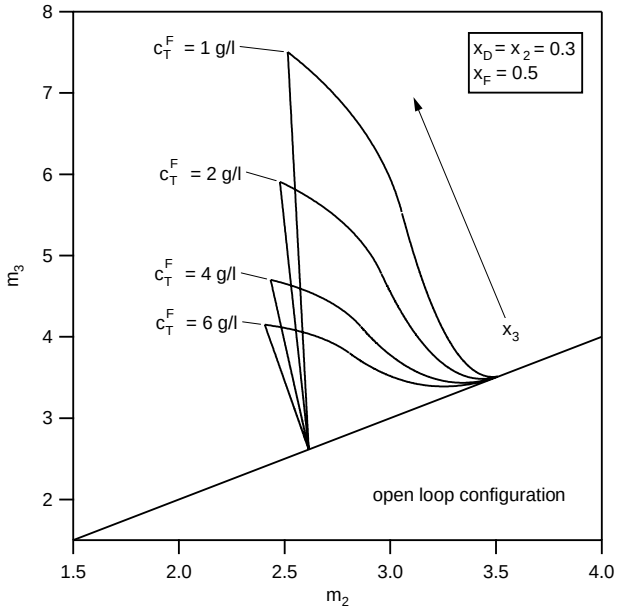

Fig. 5. In case of a nonlinear isotherm, the complete separation region for fixed x_2 depends on the feed concentration c_T^F. The area decreases with increasing feed concentration.

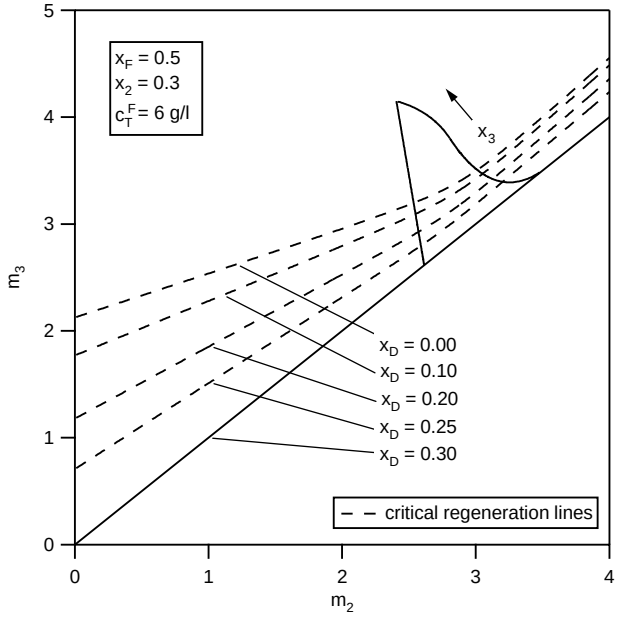

Fig. 6. Nonlinear complete separation region for fixed x_2. The dashed lines represent the critical regeneration lines for different desorbent compositions in a closed loop configuration. Only above the lines, a set of m_1 and m_4 fulfilling the regeneration constraints (Eqs. (12) and (13)), can be found. Hence, the critical regeneration line cuts off the complete separation area and detaches it from the diagonal.

under the combined effect of an increasing value of c_T^F and a decreasing value of $(m_3 - m_2)$ [16].

It is worth recalling that the triangle-shaped regions in the (m_2, m_3) plane shown in Figs. 3–5 represent a region of complete separation only under the assumption that a complete regeneration of the solid and the fluid phase in Sections 1 and 4, respectively, is achieved. This is guaranteed when the following conditions on m_1 and m_4 are fulfilled:

$$m_1 > m_1^{cr}(x_2) = H_A(x_2) \tag{12}$$

$$m_4 < m_4^{cr}(m_2, m_3, x_2, x_3) = \frac{1}{2}\left[H_B(x_3) + m_3 + k_B(x_3)c_B^F(m_3 - m_2) - \sqrt{(H_B(x_3) + m_3 + k_B(x_3)c_B^F(m_3 - m_2))^2 - 4H_B(x_3)m_3}\right] \tag{13}$$

It is worth noting that the former constraint on m_1 is the same as in the linear case, whereas the latter depends on the operating point (m_2, m_3) [16].

3.2. The 'closed loop'-configuration

In the case of an open loop configuration x_2 equals x_D, and the complete separation regions in Figs. 4 and 5 are constituted of points at constant x_F value, which fulfil Eq. (10). For a closed loop configuration, however, x_2 is usually larger than x_D, except for the limiting cases where either the recycle flow Q_4 or the feed flow Q_F approaches zero. Following the same approach as for the open loop configuration, a complete separation region can be determined for the chosen value of x_2. However, in this case, in addition to the solvent balance at the feed node (10) also the balance at the desorbent node, i.e. Eq. (8), must be fulfilled, which can be recast in terms of m_j values as follows:

$$m_1(x_2 - x_D) = m_4(x_3 - x_D) \tag{14}$$

At the same time m_1 and m_4 must comply with the constraints given by Eqs. (12) and (13)). This implies that among the operating points in the (m_2, m_3) plane associated to a given pair of modifier concentrations (x_2, x_3) only those are feasible, for which two values m_1 and m_4 can be found that fulfill Eq. (14) and at the same time Eqs. (12) and (13)). Such requirement defines implicitly a line in the (m_2, m_3) plane such that the operating points below it are not acceptable, because they violate the regeneration specifications in either Sections 1 and 4. This line depends on the chosen values of x_F and x_D as illustrated in Fig. 6, for the case of $c_T^F = 6$ g/l, $x_F = 0.5$, and various x_D values between 0 and 0.3. Such lines identify a feasible upper region in the triangle-shaped complete separation region associated to $x_2 = 0.3$. The ultimate result, i.e. the final complete separation region for a given set of external mobile phase compositions, i.e. for a given pair x_F and x_D, and for a given total feed concentration c_T^F, is obtained by combining the separation regions obtained for different values of x_2. This is illustrated in Fig. 7, for $c_T^F = 6$ g/l, $x_F = 0.5$ and $x_D = 0.25$. The complete separation region is identified by a thick boundary, and is constituted of a series of triangle-shaped regions (with thinner boundaries) associated to x_2 values between 0.25 (the

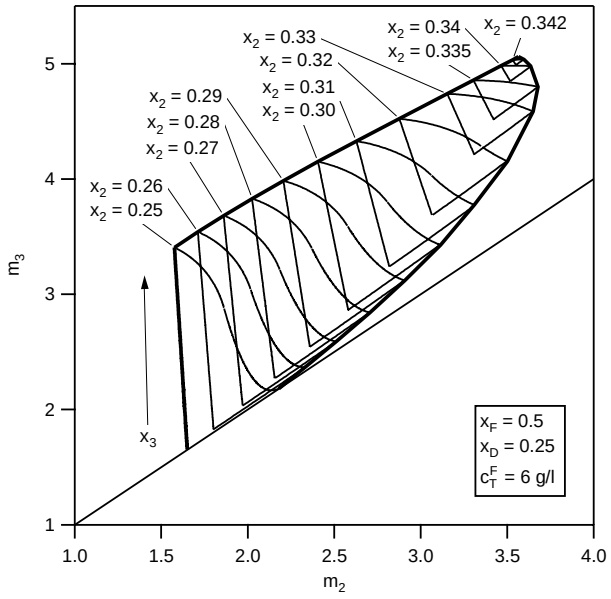

Fig. 7. Nonlinear complete separation region for different values of x_2. The complete separation region for the given pair (x_D, x_F) is obtained by combining all of them. The leftmost region, whose basis is on the diagonal, applies to the open loop configuration where $x_2 = x_D$.

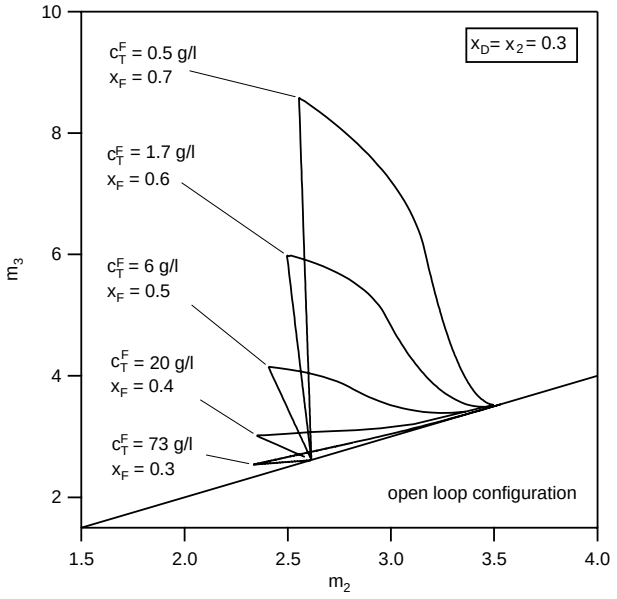

Fig. 8. Nonlinear complete separation regions at fixed $x_2 = 0.3$ for $x_F = 0.3$, 0.4, 0.5, 0.6, 0.7, each with the racemic feed concentration slightly below the corresponding solubility limit.

leftmost region) and about 0.36. Beyond this last x_2 value, the intersection between the region calculated for the chosen x_2 value and the feasible region complying with constraints (12), (13) and (14) is void. In the case shown in Fig. 7, the highest productivity and lowest desorbent requirement are achieved in the vertex of the triangle with the lowest x_2 value where the recycle flow goes to zero.

4. Discussion and conclusion

In this work we have developed tools to understand the behavior of SG–SMBs and to design their operating conditions. Next, we evaluate critically the potential of the solvent gradient operation of SMBs for practical applications. Our discussion will focus on the issue of solubility, and we will refer to the α-ionone system and the corresponding data presented in Section 2.2 and in Fig. 2.

For the sake of simplicity, but without loss of generality, let us consider the open-loop SG–SMB where the composition of the desorbent stream, i.e. x_D, and x_2 are the same and fixed. By fixing the composition of the solvent used in the feed stream, the maximum feed concentration, c_T^F, can be obtained from the curve in Fig. 2. For $x_F \geq x_D$, where $x_F = x_D$ identifies the isocratic SMB operation, the maximum solubility decreases with increasing x_F. Assuming as a reference for the analysis that c_T^F coincides with the racemate solubility, it is then possible for every pair x_F and c_T^F to determine the corresponding complete separation region in the (m_2, m_3) plane. A few such regions are drawn in Fig. 8. It can readily be observed that increasing x_F, and decreasing c_T^F accordingly, leads to larger regions, whereas values of x_F close to x_D leads to very high feed concentrations and very thin complete separation regions. The thinnest triangle in Fig. 8 corresponds to isocratic SMB operation, i.e. no gradient. With reference to the definition of productivity (11), changing x_F yields conflicting trends in the two key parameters controlling productivity, i.e. $(m_3 - m_2)$ and c_T^F. In the case under examination the effect of the feed concentration prevails and a five-fold increase of productivity in going from $x_F = 0.7$, i.e. maximum gradient, to $x_F = 0.3$, i.e. isocratic SMB, can be observed (see Table 1). This indicates that SG–SMB operation does not improve on isocratic SMB in this case, and we suspect that this might be a general trend.

However, this first result has to be considered also in view of robustness considerations. It is well known that the thinner the complete separation region the less robust the SMB operation is [16]. This implies that decreasing x_F in Fig. 8 leads to less robust operation from the point of view of the feasible region of separation. This should lead to the conclusion that there might be an optimal gradient operation,

Table 1
Comparison of feed flowrate $Q_F \propto (m_3 - m_2)$ and productivity PR $\propto (m_3 - m_2)c_T^F$ based on identical switch time t^* and identical SMB unit $(n_{col}, V, \varepsilon)$ in the vertexes of the separation areas shown in Fig. 8

x_F	c_T^F (g/l)	$(m_3 - m_2)$ (g/l)	$(m_3 - m_2)c_T^F$ (g/l)
0.3	73	0.207	15.1
0.4	20	0.666	13.3
0.5	6	1.743	10.5
0.6	1.7	3.489	5.9
0.7	0.5	6.030	3.0

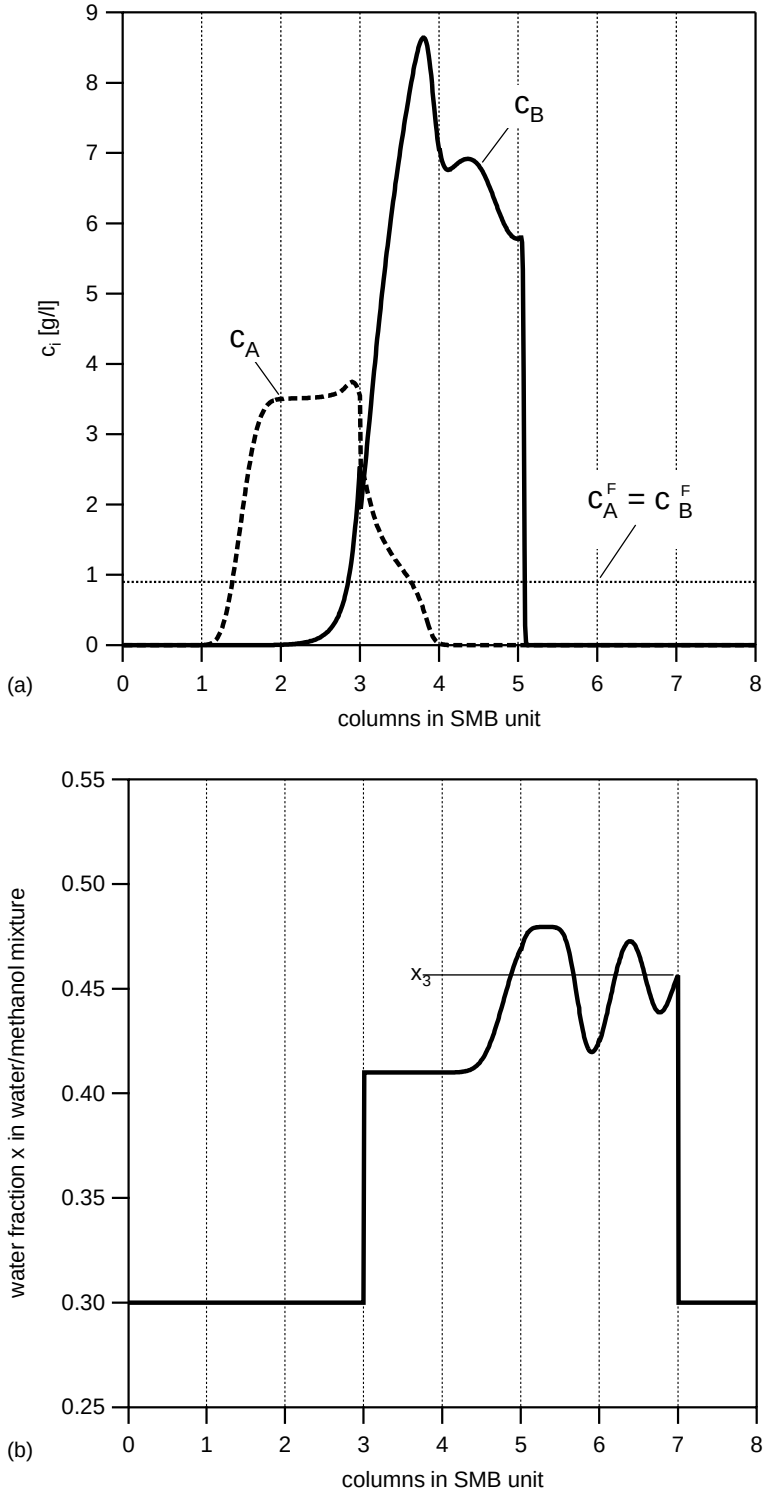

Fig. 9. Detailed simulation of an open loop SMB with $x_2 = x_D = 0.3$, $x_F = 0.6$, $m_1 = 4.3$, $m_2 = 2.63$, $m_3 = 5.5$, $m_4 = 1.8$, $\varepsilon_p = 0$, $\varepsilon^* = 0.7$, $D_A = D_B = D_W = 0.001\,cm^2/s$, $a_p k_{q,A} = a_p k_{q,B} = 10\,s^{-1}$, $V = 0.785\,ml$, $t^* = 200\,s$, $c_T^F = 1.8\,g/l$ (slightly below solubility limit for x_F), adsorption isotherms according to Eqs. (6) and (7). Internal profile just after the switch versus the position of the eight columns inside the SMB unit of: (a) concentration of A and B; (b) water fraction x.

i.e. a value of x_F that allows for the best trade-off between productivity and robustness. This could be determined only through detailed optimization, based on a proper measure of robustness.

This measure should include another important aspect of SMB operation, particularly of SG–SMB operation, namely the internal concentration profiles. It has in fact been observed [14] that solvent gradient operation of SMBs may

lead to an enrichment in the fluid phase beyond the feed concentration. An example of this is shown in Fig. 9a where the internal concentration profiles are shown, as computed with a detailed SMB model including the modifier mass balance equation (Eqs. (22) to (24) of Part I, modified to account for the Langmuir adsorption isotherm of Eq. (5)). The nominal modifier concentrations x_2 and x_3 that are calculated using the TMB model and are used for the design of the separation are $x_2 = 0.3$ and $x_3 = 0.457$. The former coincides with the correct value for the SMB unit, whereas the latter is only an approximation of the real water concentration profile, which is shown in Fig. 9b. The solubility value corresponding to x_2 is extremely high, whereas that corresponding to the nominal x_3 value, i.e. 10 g/l, is very close to the actual c_B concentration in section 3. This raises the question whether there might be solubility problems within the SMB columns in the gradient mode operation, that might completely spoil the separation. It is difficult to answer this question in general terms since this is very much system-specific, and depends also on the detailed solid/liquid equilibrium of the two enantiomers in the mixed solvent system. In general in fact pure enantiomers have a different solubility, either higher or lower than the racemate.

The general conclusion to be drawn based on the analysis above is that the technical feasibility and attractiveness of solvent gradient SMBs depend on a rather delicate compromise between conflicting requirements and constraints. Feasibility should be assessed through detailed optimization. However, such optimization requires an amount of rather detailed information about retention and solubility at different mobile phase compositions, that goes beyond what is normally required for isocratic SMB design.

5. Nomenclature

a	fitting parameter in Eq. (7)
a_p	specific surface of the adsorbent particles (cm^{-1})
c	concentration, (g/l)
D	axial dispersion coefficient, (cm^2/s)
h	fitting parameter in Eq. (6)
H	Henry's constant
k	Langmuir parameter (l/g)
k_q	mass transfer coefficient in the lumped pore diffusion model (cm/s)
m	flowrate ratio
n	fitting parameter in Eq. (6)
n_{col}	number of columns in the SMB
PR	purity
q	adsorbed phase concentration (g/l)
q^*	adsorbed phase concentration in equilibrium (g/l)
Q	volumetric fluid flowrate (ml/min)
Q_s	volumetric solid flowrate (ml/min)
t	time (s)
t^*	switch time (s)
V	volume of one column (ml)
x	volume fraction of the weaker solvent (e.g. water in a water/methanol mixture)
z	axial coordinate (cm)

Greek letter

ε	bed void fraction

Subscripts and superscripts

A	more retained component
B	less retained component
cr	critical value
D	desorbent
E	extract
F	feed
i	component index ($i = A, B$)
j	section index ($j = 1, \ldots, 4$)
P	at operating point P
R	raffinate
SMB	Simulated Moving Bed
TMB	True Moving Bed
W	weaker solvent in the fluid phase (e.g. water in a water/methanol mixture)
0	reference value at $x = 0$

Acknowledgements

The partial support of the Research Commission of ETH Zurich through grant TH-23′/00-1 is gratefully acknowledged.

References

[1] M. Juza, M. Mazzotti, M. Morbidelli, Trends Biotechnol. 18 (2000) 108.
[2] R.M. Nicoud, in: G. Subramanian (Ed.), Bioseparation and Bioprocessing, Wiley-VCH, New York, 1998.
[3] O. Ludemann-Hombourger, R.M. Nicoud, M. Bailly, Sep. Sci. Technol. 35 (2000) 1829.
[4] O. Ludemann-Hombourger, G. Pigorini, R.M. Nicoud, D.S. Ross, G. Terfloth, J. Chromatogr. A 947 (2002) 59.
[5] E. Kloppenburg, E.D. Gilles, Chem. Eng. Technol. 22 (1999) 10.
[6] Y. Zang, P.C. Wankat, Ind. Eng. Chem. Res. 41 (2002) 2504.
[7] Z. Zhang, M. Mazzotti, M. Morbidelli, J. Chromatogr. A 1006 (2003) 87.
[8] C. Migliorini, M. Wendlinger, M. Mazzotti, Ind. Eng. Chem. Res. 40 (2001) 2606.
[9] J.Y. Clavier, M. Perrut, R.M. Nicoud, in: Ph. Rudolf von Rohr, Ch. Trepp (Eds.), High Pressure Chemical Engineering, Elsevier, London, 1996.
[10] O. DiGiovanni, M. Mazzotti, M. Morbidelli, F. Denet, W. Hauck, R.M. Nicoud, J. Chromatogr. A 919 (2001) 1.
[11] F. Denet, W. Hauck, R.M. Nicoud, O. DiGiovanni, M. Mazzotti, J.-N. Jaubert, M. Morbidelli, Ind. Eng. Chem. Res. 40 (2001) 4603.
[12] T.B. Jensen, T.G.P. Reijns, H.A.H. Billiet, L.A.M. van der Wielen, J. Chromatogr. A 873 (2000) 149.

[13] D. Antos, A. Seidel-Morgenstern, Chem. Eng. Sci. 56 (2001) 6667.
[14] S. Abel, M. Mazzotti, M. Morbidelli, J. Chromatogr. A 944 (2002) 23.
[15] J. Houwing, H.A.H. Billiet, L.A.M. van der Wielen, J. Chromatogr. A 944 (2002) 189.
[16] M. Mazzotti, G. Storti, M. Morbidelli, J. Chromatogr. A 769 (1997) 3.
[17] F. Quattrini, G. Biressi, M. Juza, M. Mazzotti, C. Fuganti, M. Morbidelli, J. Chromatogr. A 865 (1999) 201.
[18] G. Zenoni, F. Quattrini, M. Mazzotti, C. Fuganti, M. Morbidelli, Flavour Frag. J. 17 (2002) 195.